INTERNATIONAL JOURNAL FOR NUMERICAL METHODS IN FLUIDS
Int. J. Numer. Meth. Fluids 2007; **53**:1005–1018
Published online 23 August 2006 in Wiley InterScience (www.interscience.wiley.com). DOI: 10.1002/fld.1317

A piecewise linear approach to volume tracking a triple point

Benjamin Y. Choi[‡] and Markus Bussmann[*,†]

Department of Mechanical and Industrial Engineering, University of Toronto, 5 King's College Road, Toronto, Ont., Canada M5W 3G8

SUMMARY

An approach to volume tracking three materials is presented that, in contrast with the so-called 'onion-skin' methodology, assumes the existence of a 'triple point' at which two interfaces between three materials intersect. The reconstruction of any cell that contains three materials is iterative: the approach is to locate a point of intersection between two interfaces that minimizes a given error expression. The advantages and limitations of the algorithm are presented via a series of advection tests that demonstrate that triple points can be reconstructed and advected just as well as simpler interfaces in typical applications. Copyright © 2006 John Wiley & Sons, Ltd.

Received 22 December 2005; Revised 24 June 2006; Accepted 27 June 2006

KEY WORDS: volume tracking; VOF; piecewise linear; triple point; PLIC; multi-material

1. INTRODUCTION

Volume tracking is a popular approach to interface tracking, usually based on a piecewise-linear (PLIC) reconstruction of interfaces between two fluids, as illustrated in Figure 1. An actual interface (Figure 1(a)) between two fluids is represented by values of a scalar volume fraction (Figure 1(b)) that represent the fraction of each cell volume occupied by (in this case) fluid 1. Figure 1(c) is a depiction of a reconstructed interface: for each cell that contains some of each of the two fluids, the orientation of the interface is estimated, and the interface is reconstructed with a linear (planar in 3D) segment that exactly corresponds to the known volume fraction. Following reconstruction, volume fractions are advected (Figure 1(d)) from one timestep to the next according to any of a variety of advection schemes, based on the reconstructed geometry in order to maintain a sharp interface representation.

*Correspondence to: Markus Bussmann, Department of Mechanical and Industrial Engineering, University of Toronto, 5 King's College Road, Toronto, Ont., Canada M5W 3G8.
†E-mail: bussmann@mie.utoronto.ca
‡E-mail: ben.choi@utoronto.ca

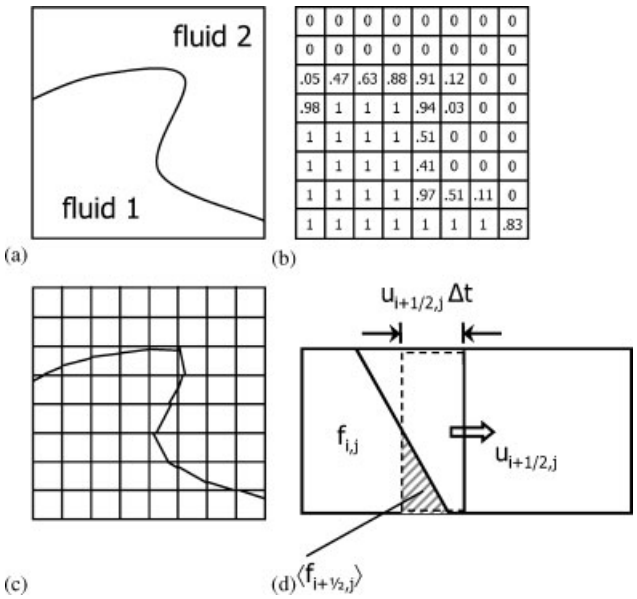

Figure 1. (a) An interface between two fluids; (b) the corresponding volume fractions of fluid 1; (c) the piecewise linear reconstruction of the interface; and (d) the geometric advection of fluid volume $\langle f_{i+1/2,\,j} \rangle$ from one cell to another.

Numerous papers describe volume tracking algorithms (e.g. References [1–5]) that typically differ in the approach to calculating interface orientation and/or the advection step. And while volume tracking may not be an appropriate algorithm for all interface tracking requirements—for example, surface tension-dominated flows can be difficult to model accurately because the volume fraction field does not readily yield accurate estimates of curvature—the method nevertheless has been successfully applied to a variety of applications (e.g. References [6–8]).

But what happens when there are more than two fluids in a domain, and in particular, when two interfaces between three fluids meet at a contact line, or in 2D, at a 'triple point', as illustrated in Figure 2? Such a configuration will appear, for example, whenever a dispersed phase in the form of a drop or bubble interacts with an interface between two other fluids; such contact line phenomena occur in a variety of chemical and metallurgical processes. While many papers introduce volume tracking as a methodology for any number of fluids, the algorithms that have been developed are almost always for the simplest case of two.

The only approach to multi-fluid volume tracking that the authors are aware of is the so-called 'onion-skin' method for reconstructing layered materials, originally presented by Noh and Woodward [1], extended to a PLIC reconstruction by Youngs [2], reviewed by Benson [9], and illustrated in Figure 3. For a cell containing n materials, with the order of reconstruction prescribed *a priori* (an alternative is to determine the order as part of the calculation procedure [10–12]), the interface between materials k and $k+1$ is defined as the interface between the sum of the volume fractions of materials $1, 2, \ldots, k$, and the sum of the volume fractions of materials $k+1, k+2, \ldots, n$. Each interface orientation and position can then be determined by any technique developed for a two-material configuration.

DOI: 10.1002/fld

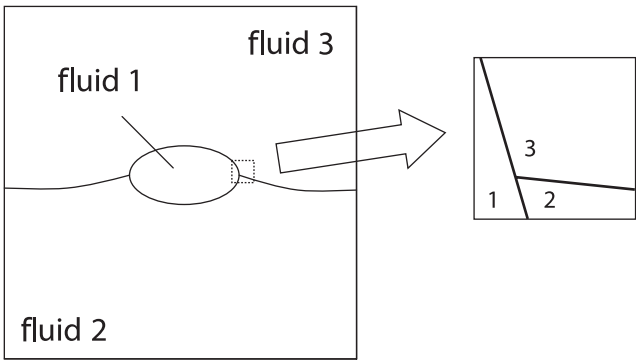

Figure 2. An example of a three-fluid configuration, with interfaces between pairs of fluids, and a triple point at the intersection of interfaces. When discretized, a domain will include cells that contain three materials, as illustrated in the close-up.

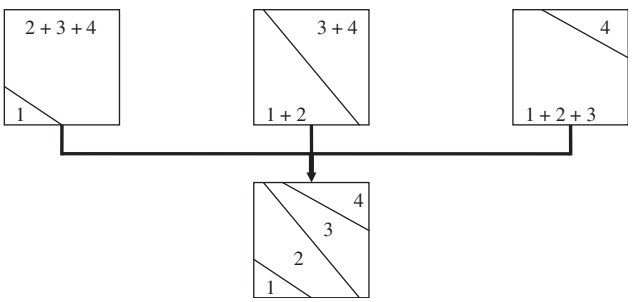

Figure 3. The onion-skin method for reconstructing three interfaces between four layered materials.

The onion-skin method is appropriate for the reconstruction of layered materials, but it cannot be used to represent a junction point at which three materials meet. Consider the T junction of Figure 4(a), and the corresponding volume fractions in a 3×3 stencil illustrated in Figure 4(b). The three materials are denoted 1, 2 and 3, and reconstructed in that order. Two normals are also defined: $\mathbf{n}_1$ as the normal pointing out from material 1, and $\mathbf{n}_{2,3}$ as the normal to the interface between materials 2 and 3, pointing towards material 3.

If one were to reconstruct this configuration via the onion-skin method, with normals calculated using the finite difference expression of Parker and Youngs [13], the calculated normals would be $\mathbf{n}_1 = 2\hat{j}$ and $\mathbf{n}_{2,3} = \hat{i} + \hat{j}$ (where $\hat{i}$ and $\hat{j}$ are the unit vectors in the x- and y-directions), and the reconstruction would appear as in Figure 4(c). Although $\mathbf{n}_1$ is accurately estimated, it is clear that the onion-skin model not only yields a poor estimate of $\mathbf{n}_{2,3}$, but the deviation between the calculated and exact orientations demonstrates a fundamental limitation of this method: the reconstructed interfaces can intersect, unlike those of an onion-skin, and the reconstruction then no longer corresponds to the specified volume fractions, which in turn will lead to incorrect volume flux estimates during the advection step.

DOI: 10.1002/fld

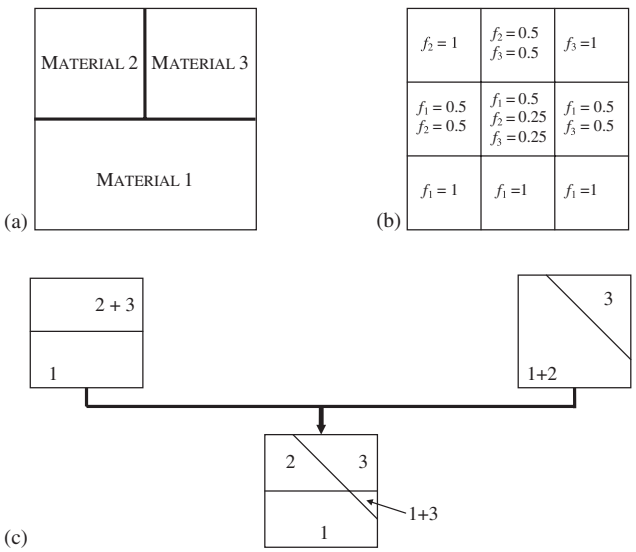

Figure 4. (a) A T configuration of three materials; (b) the corresponding volume fractions; and (c) the onion-skin reconstruction of this configuration. Note that when interfaces intersect, the reconstruction no longer corresponds to the specified volume fractions.

In this paper we present an alternative: a PLIC methodology for reconstructing a three-material configuration that allows for the existence of a triple point. The methodology and results we present are in 2D, although the extension to 3D is conceptually no more difficult, if significantly more complicated to implement. But the same can be said of geometric volume tracking algorithms in general: the extension to 3D usually involves much more complicated geometry.

The algorithm is described in Section 2, the results of various tests are presented in Section 3, and the paper is summarized in Section 4.

2. VOLUME TRACKING THREE MATERIALS

In what follows we describe an approach to reconstructing a three-material cell that accurately estimates interface normals, determines the position of a triple point if it exists, and exactly conserves mass. Part of the methodology is based on the onion-skin model of Youngs [2]: given materials 1, 2 and 3, the orientation of the interface that confines material 1 (interface$_1$) is calculated as the normal to the interface between material 1 and the sum of materials 2 and 3, via the expression of Parker and Youngs [13]. But unlike the onion-skin method, the position of the second interface that divides materials 2 and 3 (interface$_{2,3}$) is determined by a minimization procedure similar to the LVIRA algorithm of Pilliod and Puckett [14]. As to the choice of material 1, it was mentioned previously that algorithms have been developed that determine the order of reconstruction based on the configuration of nearby fluid [10–12]. We did not implement any of these. Instead, considering the contact line phenomena that are of interest to us, for the results presented in this paper, we could identify a so-called 'dispersed' phase consisting of one or two materials: if one, we designated that material as 1; if two, we designated the other (third) material as material 1.

DOI: 10.1002/fld

In the following section, we briefly review the equations for two-fluid volume tracking, and then present the methodology for three materials.

2.1. A brief review of Youngs' method [2] for volume tracking two materials

Referring again to Figure 1(b), consider that volume fractions of fluid 1 are known at a time t^n. These volume fractions are discrete values of a continuous indicator (or colour) function f (equal to one within fluid 1, and zero elsewhere) that is advected with the flow:

$$\frac{\partial f}{\partial t} + \nabla \cdot (\mathbf{u} f) = 0 \tag{1}$$

Youngs [2] discretized the equation in a split manner:

$$\begin{aligned} f^*_{i,j} &= \frac{f^n_{i,j} V_{i,j} - [u_{i+1/2,j} \langle f^n_{i+1/2,j} \rangle - u_{i-1/2,j} \langle f^n_{i-1/2,j} \rangle] \Delta y \Delta t}{V^*_{i,j}} \\ f^{n+1}_{i,j} &= \frac{f^*_{i,j} V^*_{i,j} - [v_{i,j+1/2} \langle f^*_{i,j+1/2} \rangle - v_{i,j-1/2} \langle f^*_{i,j-1/2} \rangle] \Delta x \Delta t}{V_{i,j}} \end{aligned} \tag{2}$$

where $\Delta t = t^{n+1} - t^n$, u and v are normal velocities to cell faces, $V_{i,j}$ is the cell volume, $V^*_{i,j} = V_{i,j} - (u_{i+1/2,j} - u_{i-1/2,j}) \Delta y \Delta t$, and the quantities in $\langle\,\rangle$ are fluxed volumes. The order of advection is alternated from one timestep to the next, to minimize directional bias.

The fluxed volumes are calculated geometrically. For each cell (i, j) that contains an interface, the normal $\mathbf{n} = \nabla f = (f_x, f_y)$ to the interface is evaluated via the finite difference expression of Parker and Youngs:

$$f_x = \frac{(f_{i+1,j+1} + 2 f_{i+1,j} + f_{i+1,j-1}) - (f_{i-1,j+1} + 2 f_{i-1,j} + f_{i-1,j-1})}{8 \Delta x} \tag{3}$$

with an analogous expression for f_y, where the subscripts in Equation (3) refer to a 3×3 stencil of cells about (i, j). The normal is then used to position a line segment within each interface cell that exactly corresponds to the known volume fraction in that cell. From that reconstruction, the fluxed volumes can then be calculated, as illustrated in Figure 1(d).

2.2. Methodology for volume tracking three materials

For a three-fluid problem with a triple point, a domain will contain one or more cells that contain all three materials, and a proper reconstruction of such cells is crucial to ensuring that the triple point remains well resolved, rather than diffusing into neighbouring cells. Our algorithm for reconstructing a cell that contains three materials begins as does the onion-skin method, by reconstructing interface$_1$, the interface between material 1 and the sum of materials 2 and 3, by calculating $\mathbf{n}_1$ via Equation (3). For the simple T junction of Figure 4, interface$_1$ is reconstructed exactly. In most cases, the reconstruction is not exact, but nevertheless reasonably accurate.

What remains is to determine the normal $\mathbf{n}_{2,3}$ that is required to reconstruct interface$_{2,3}$. At this point, it is important to recognize that a three-material cell need not contain a triple point, but may be a cell near another that contains a triple point. Figure 5 illustrates the distinction: cell (a) contains a triple point, and so interface$_1$ intersects interface$_{2,3}$ within the cell; in cell (b), on the other hand, the two interfaces do not intersect.

DOI: 10.1002/fld

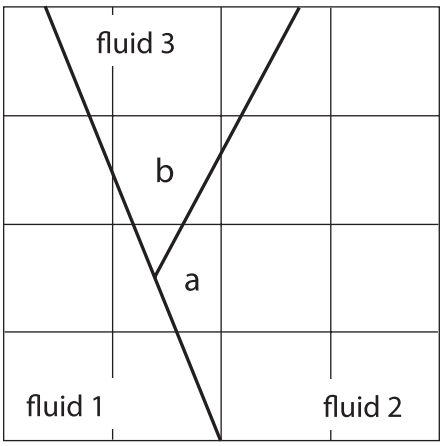

Figure 5. A three-fluid configuration that includes two cells that each contain all three fluids: (a) contains a triple point, while (b) neighbours a cell with a triple point.

To calculate $\mathbf{n}_{2,3}$ in a three-material cell, interface$_{2,3}$ is assumed to be not parallel to interface$_1$, so that the two interfaces will intersect either inside the cell (cell (a) of Figure 5) or outside the cell, if the two interfaces were extrapolated beyond the cell faces (cell (b)). The normal $\mathbf{n}_{2,3}$ is then calculated by determining a point of intersection of the two interfaces, based on position z along interface$_1$, subject to the constraint that interface$_{2,3}$ divide the cell into volumes that correspond to the known volume fractions of materials 2 and 3. The actual choice of the point of intersection of the two interfaces is determined by minimizing the following function:

$$g(z) = \sum_{i,j} [(f2_{i,j} - f2^p_{i,j})^2 + (f3_{i,j} - f3^p_{i,j})^2] \tag{4}$$

where $f2_{i,j}$ and $f3_{i,j}$ are the actual volume fractions of materials 2 and 3 in a 3×3 stencil about a three-material cell, and $f2^p_{i,j}$ and $f3^p_{i,j}$ are the volume fractions based on the *predicted* geometry, that are a function of z. In our implementation we minimized $g(z)$ using a modified version of the Golden Section Search [15]: the range of z was limited to nine cell widths on either side of the three-material cell, and the search for a minimum allowed for convergence at either of the end points. The search was done twice, for materials 2 and 3 on either side of interface$_{2,3}$, and the absolute minimum chosen.

For each value of z evaluated during the minimization, the implementation of this algorithm requires the evaluation of various geometric constructs to determine the position of interface$_{2,3}$. These were implemented via the 'geometric toolbox' of Rider and Kothe [3]; further details will not be presented here.

Given a three-material reconstruction that includes two interfaces, the second part of volume tracking is the advection step. The geometry is somewhat more complicated than for the simpler case of one interface within a cell (as illustrated in Figure 1(d)), because a fluxed volume may contain fractions of three fluids. As with the reconstruction step, the geometric calculations were implemented according to Rider and Kothe [3].

DOI: 10.1002/fld

Table I. Calculated errors, corresponding to Equation (5), for the results presented in Figures 6 and 9–11.

Figure 6—layered interfaces in rotation	Onion-skin	0.03250
	Present method	0.03252
Figure 9—compound circles in rotation	Diagonal	0.00347
	Horizontal	0.00357
	Vertical	0.00516
Figure 10—compound circles in vortical flow (1000 timesteps forward and back)	Diagonal	0.01367
	Horizontal	0.01663
	Vertical	0.01187
Figure 11—compound circles in vortical flow (2000 timesteps forward and back)	Diagonal	0.04816
	Horizontal	0.06448
	Vertical	0.06358

3. RESULTS AND DISCUSSION

We now present the results of several tests of this three-material algorithm, beginning with a layered configuration of materials without a triple point, and then various triple point configurations in translation, rotation, and shear.

The results are primarily qualitative, as the point here is to demonstrate the efficacy and limitations of the approach. For the results we present, the vast majority of reconstructions are of two materials, that we do with the algorithm of Youngs [2]. The contribution here is the approach to reconstructing the very few cells that contain three materials. As a result, the accuracy of the methodology is very similar to that of Youngs [2], which is known to be a first-order accurate technique [14, 16]. Nevertheless, we did calculate the following L1 error for most of the calculations that we ran:

$$E = \frac{\sum_{i,j} |f2^n_{i,j} - f2^e_{i,j}| + \sum_{i,j} |f3^n_{i,j} - f3^e_{i,j}|}{\sum_{i,j} f2^e_{i,j} + \sum_{i,j} f3^e_{i,j}} \tag{5}$$

where the summations are over all cells in a domain. The values are presented in Table I. Note that this is a modified version of a common expression [16] used for two-material calculations. The superscript n refers to the calculated volume fractions at the end of a simulation, and the superscript e refers to the corresponding exact values. It should also be noted that all of the velocity fields are exactly divergence-free, and since the advection algorithm is flux-based, the volume of each material is conserved to machine precision.

Figure 6 illustrates the results of a comparison of the new algorithm with the onion-skin method, for the reconstruction of three materials without a triple point. Two circles are initialized, a small one within a larger one, where the minimum distance between them is a half-cell width, which results in one or more cells that contain all three materials. This configuration is rotated once about the centre of the domain; initial and final views of both calculations are presented, both in their entirety and close-up. Qualitatively, the differences are very subtle; the corresponding errors E in Table I are equally similar.

DOI: 10.1002/fld

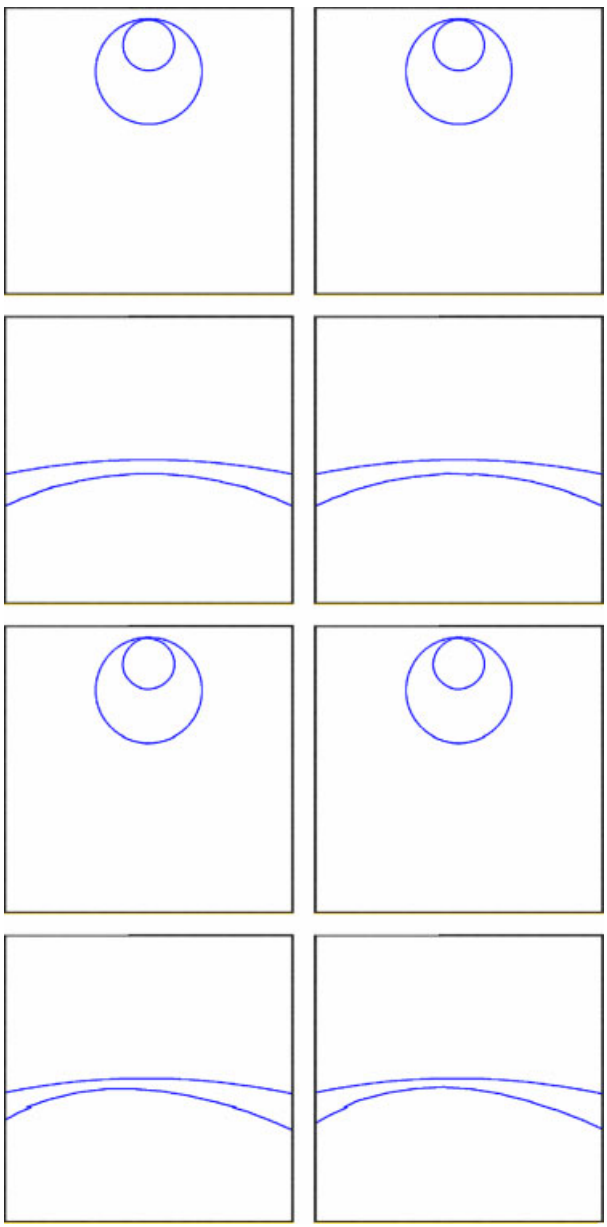

Figure 6. Layered interfaces in solid body rotation. The centre of the larger circle is 37.5 cells above the centre of rotation; the diameter of the larger circle is 50 cells. The centre of the smaller circle is 12.5 cells above the centre of the larger circle, and its diameter is 24 cells, so that the two interfaces are 0.5 cells apart. One complete rotation occurs in 2513 timesteps. The figures in the left and right columns correspond to the onion-skin method and the method presented in this paper, respectively. The first two views in each column are of the initial configuration; the third and fourth views of the final configuration.

DOI: 10.1002/fld

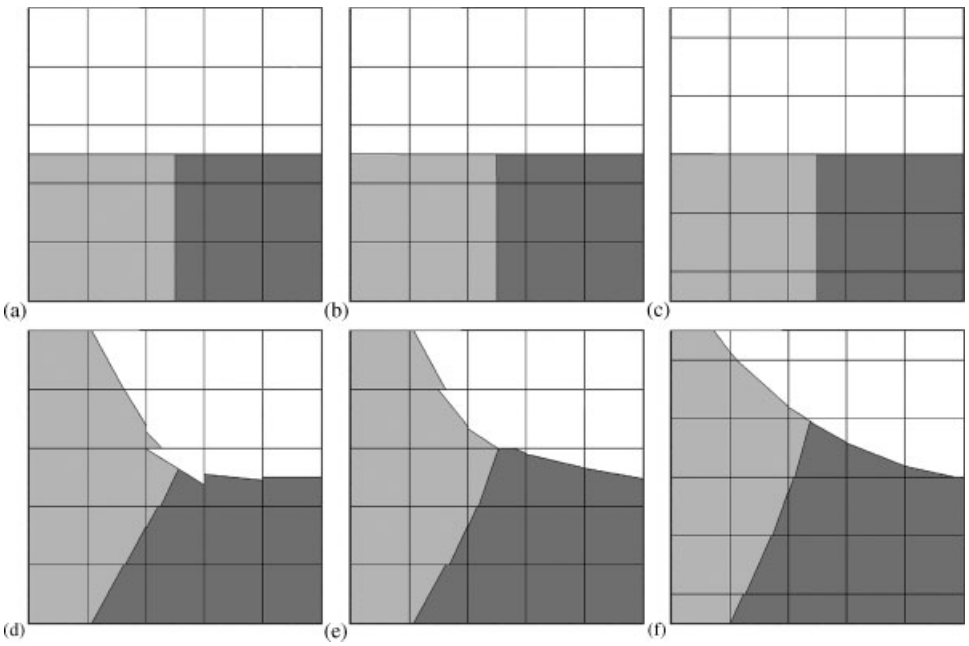

Figure 7. T and Y junctions in translation: (a) and (d) illustrate the initial configurations; (b) and (e) are the reconstructions after translation along mesh lines ($(u, v) = (1, 0)$); and (c) and (f) after translation across the mesh ($(u, v) = (2, 1)$). Each translation was for 500 timesteps at a Courant number of 0.25 (based on the u velocity).

The remainder of the results are of material configurations that include a triple point, for which the onion-skin model is ill suited. To begin, Figure 7 illustrates the results of four tests: the translation of T and Y junctions, each along the mesh and across it. In each case, material 1 (reconstructed first) is white; materials 2 and 3 are depicted by shades of grey. Figures 7(a) and (d) are of the initial configurations: the T is reconstructed exactly, while the Y (corresponding to three 120° sectors) is not, and cannot be, given the methodology as presented, because material 1 is reconstructed first in a piecewise linear manner, and so is assumed to be a material defined by a continuous interface. In that sense, the Y advection results illustrate a type of triple point that the algorithm is not designed to reconstruct.

Figures 7(b) and (e) illustrate the T and Y junctions, respectively, after translation for 125 cells horizontally along the mesh; Figures 7(c) and (f) illustrate the junctions after translation across the mesh: 125 cells to the right and 62.5 cells up. The T junction is translated exactly in each case, as it should be, because the junction can be exactly reconstructed in a piecewise linear manner. The Y junction, on the other hand, slowly evolves from a Y to a T, as is especially apparent in Figure 7(f), and as one would expect since the algorithm, as designed, cannot exactly reconstruct the Y.

Figure 8 illustrates the same two initial configurations: T and Y junctions centred within a cell, but this time in solid body rotation about the triple point itself. Figures 8(b) and (e) illustrate the triple point after one complete rotation (in 503 equal timesteps); Figures 8(c) and (f) after two rotations. This time, unlike in translation, the T junction is not advected exactly; nevertheless, the T remains well resolved even after two rotations. Similarly, the Y junction retains a form very

DOI: 10.1002/fld

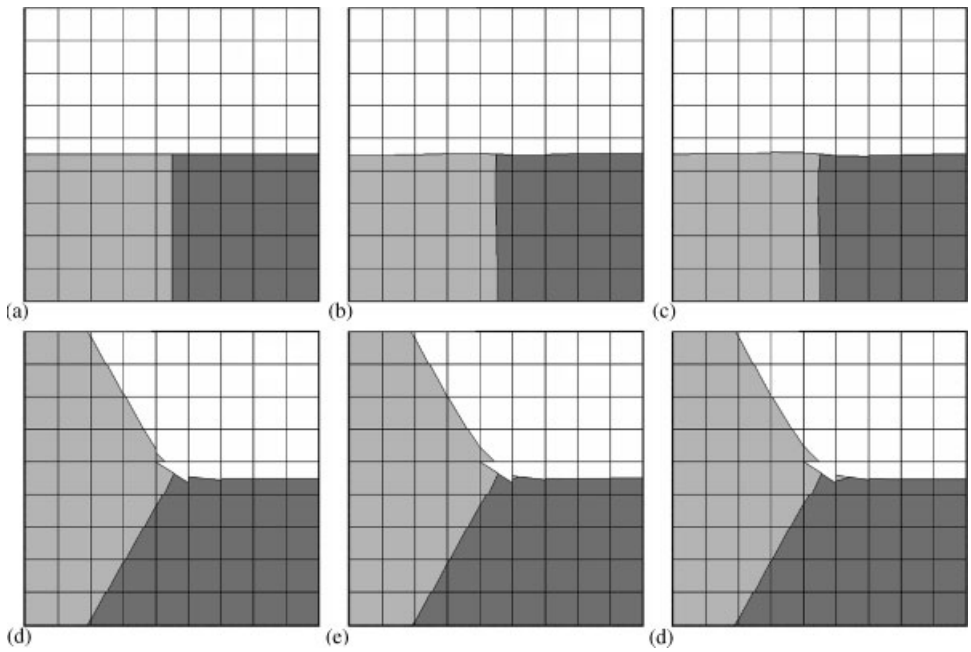

Figure 8. T and Y junctions in solid body rotation about the triple point: (a) and (d) illustrate the initial configurations; (b) and (e) the configurations after one complete rotation; and (c) and (f) after two. Each rotation was divided into 503 timesteps.

similar to that of the initial reconstruction, although it should be noted that in this case, the rotation results in the creation of a second three-material cell (to the right of the original).

Figure 9 is also of triple points in rotation, but this time the triple points are formed by halving a circle into materials 2 and 3; the surrounding material is denoted 1, and is reconstructed first. Three circles, divided horizontally, vertically, and at a 26.6° angle, are advected once about a centre of rotation outside the circle, and as Figure 9 illustrates, the triple points remain well resolved regardless of orientation.

Finally, Figures 10 and 11 present results of a modified version of an advection test [16] that combines both rotation and shear in a vortical flow that is often used to evaluate volume tracking algorithms. As before, two halves of a circle are defined, where the interface between the halves is oriented in three ways. Corresponding exactly to the test of Rudman [16], the flow field is advected N steps forward before reversing the velocities and advecting another N steps back. If the advection were exact, the initial and final configurations would be exactly the same.

Figure 10 illustrates the results for $N = 1000$, when the sheared circle is still relatively well resolved even at its maximum deformation. The initial orientation of the line that divides the circle then determines the positions of the two triple points at maximum deformation. Upon returning to the initial position, all three halved circles, including the triple points, are still well resolved, if not exactly as they were initially.

Figure 11 illustrates the results for $N = 2000$, which is a somewhat underresolved calculation. This time, the tail of the sheared circle breaks up, and the state of the triple points at the end of the

DOI: 10.1002/fld

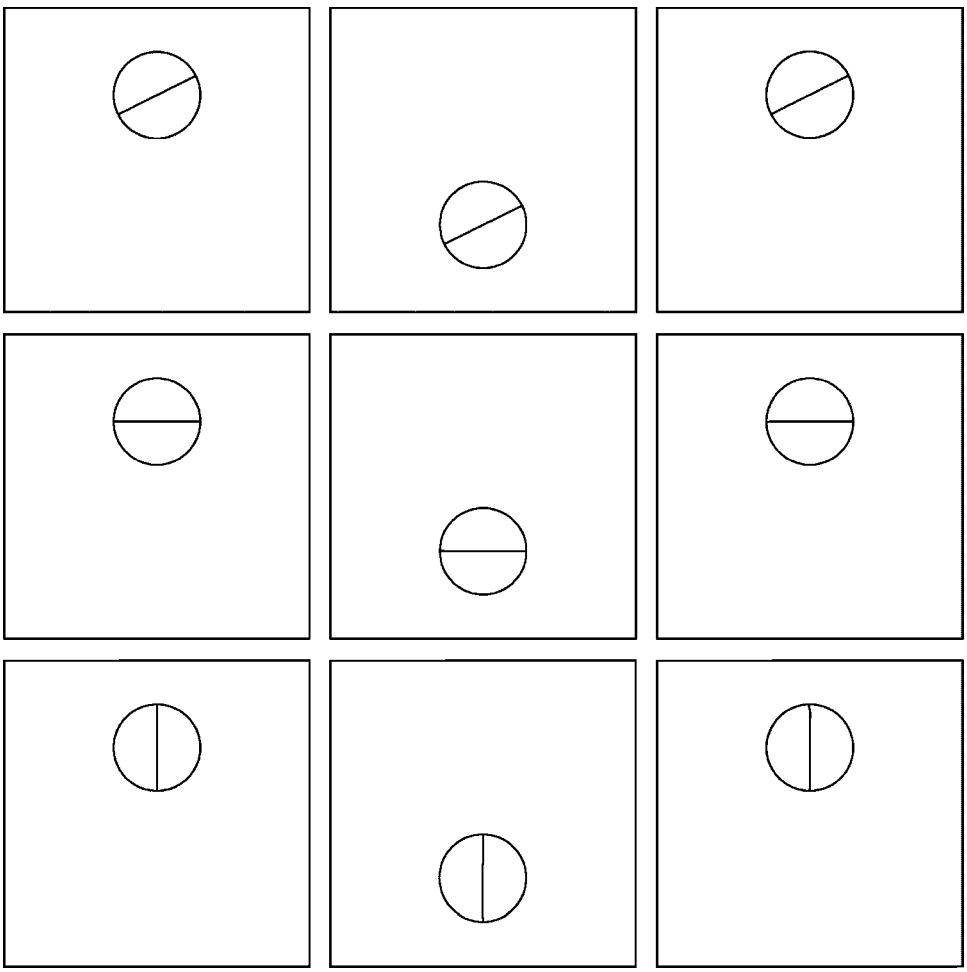

Figure 9. Compound circles in solid-body rotation. The figures in the left column are three different initial configurations; the centre and right columns illustrate the circles after a half and a full rotation about the centre of the domain. The domain is subdivided into 175×175 cells, the centre of each circle is 37.5 cells above the centre of the domain, the diameter of each circle is resolved by 50 cells, and each half rotation occurs in 1257 timesteps.

test depends very much on the initial orientation of the line that halves the circles. In particular, when the dividing line is vertical, as in the last set of results in Figure 11, one of the triple points is in the tail, so that upon returning to the initial configuration, the halved droplet is no longer clearly resolved, and bits of material 2 and 3 have collected at the bottom of the circle. On the other hand, the other five triple points in Figure 11 remain well resolved, if not entirely as they were initially, and demonstrate that this approach to volume tracking three materials does yield triple points that are as well resolved as any two fluid interfaces in a domain.

DOI: 10.1002/fld

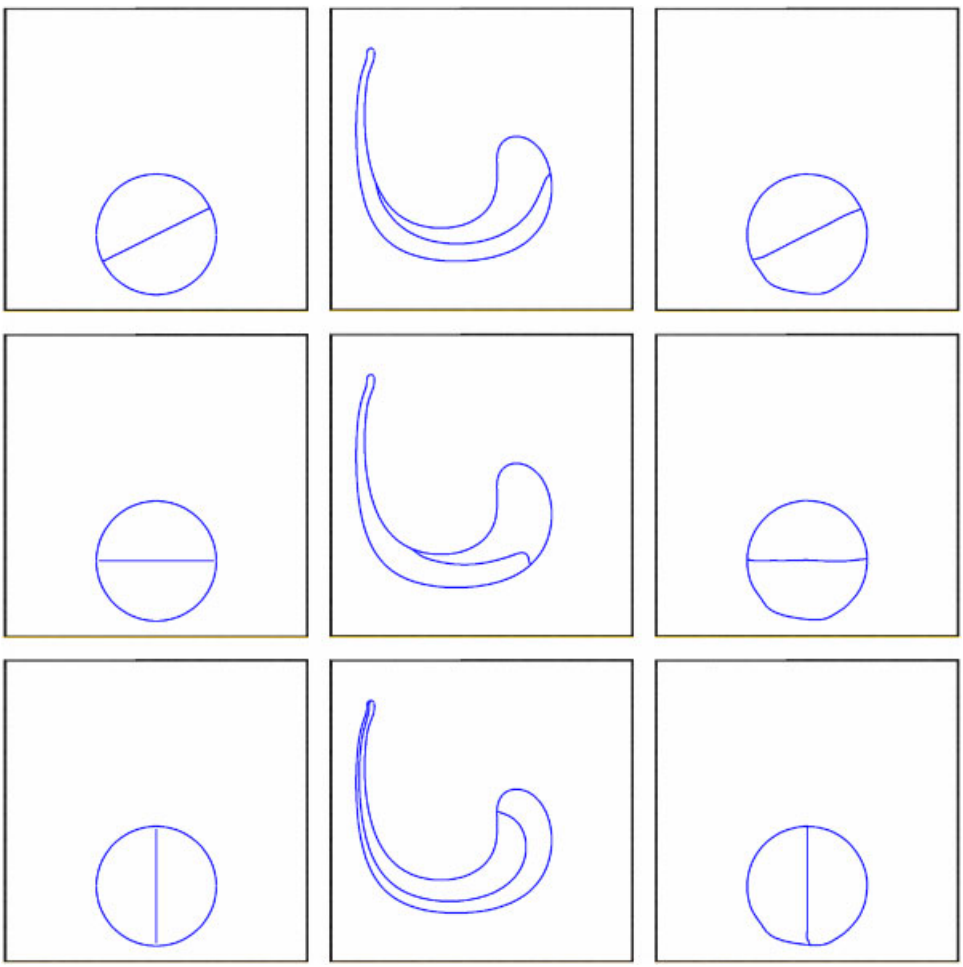

Figure 10. Compound circles in a vortical flow $V = -\sin(\pi x)\cos(\pi y)\hat{i} + \cos(\pi x)\sin(\pi y)\hat{j}$. The unit domain is discretized by 100×100 cells; the initial circle diameter is resolved by 40 cells, and the centre of the circle is initially at $(x, y) = (0.5, 0.25)$. The initial configurations are illustrated in the left column, the results after 1000 timesteps in the centre column, and then reversing the velocity field, the circles should return to their initial configurations in the right column.

4. SUMMARY

In this paper we have introduced an approach to volume tracking triple points that can easily be incorporated into any algorithm for two-fluid volume tracking; here the approach has been demonstrated in conjunction with the well-known methodology of Youngs [2]. In contrast to the only existing approach for treating more than two materials in a cell—the so-called 'onion-skin' method for reconstructing layered materials—the approach here assumes the existence of a triple point, whether in a cell that contains three materials, or in a neighbouring one. The methodology is iterative: it locates a point of intersection between two interfaces that minimizes an error expression,

DOI: 10.1002/fld

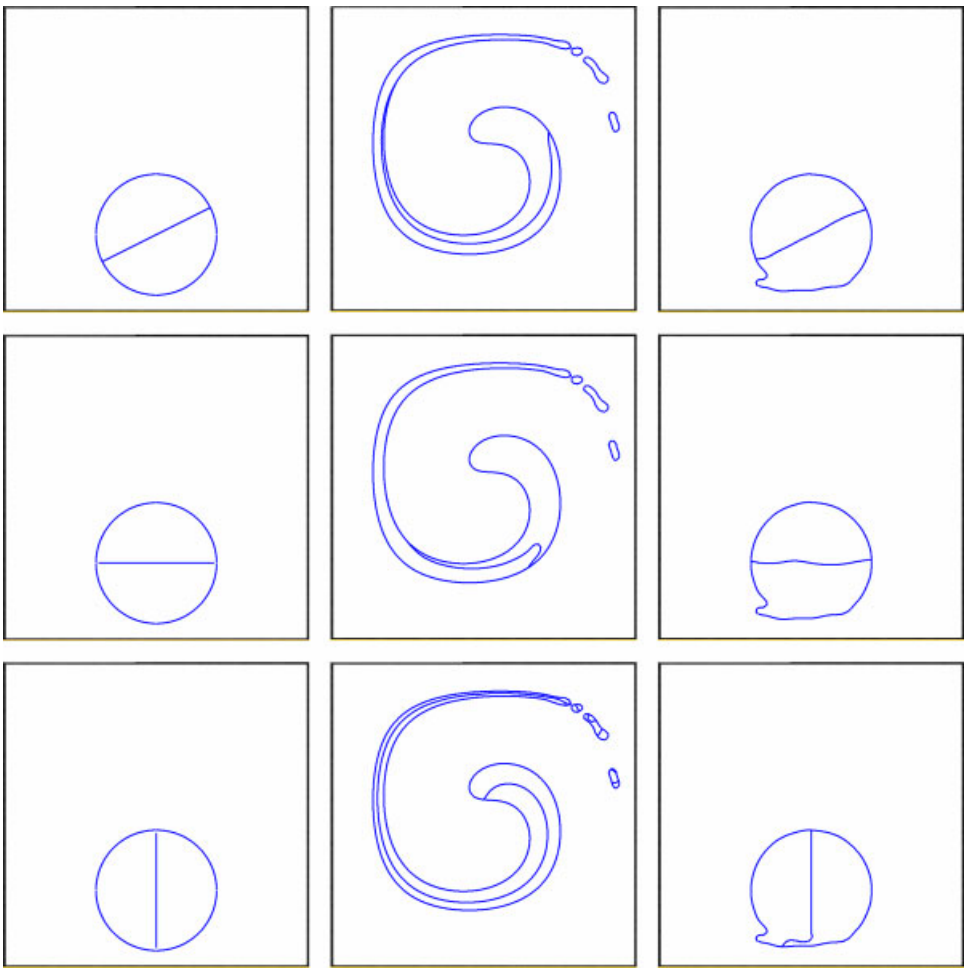

Figure 11. Similar to Figure 10, but this time the results are for 2000 timesteps forward, followed by 2000 timesteps back.

but the algorithm is only invoked for cells with three materials. By way of various advection tests, the algorithm is shown to maintain sharp representations of triple points in translation, rotation, and shear, and qualitatively at least, reconstructs and advects triple points about as well as neighbouring two fluid interfaces.

REFERENCES

1. Noh WF, Woodward P. SLIC (Simple line interface calculation). In *Lecture Notes in Physics*, van de Vooren AI, Zandbergen PJ (eds). Springer: Berlin, 1976; **59**:330–340.
2. Youngs DL. Time-dependent multi-material flow with large fluid distortion. In *Numerical Methods for Fluid Dynamics*, Morton KW, Baines MJ (eds). Academic Press: New York, 1982; 273–285.
3. Rider WJ, Kothe DB. Reconstructing volume tracking. *Journal of Computational Physics* 1998; **141**:112–152.

DOI: 10.1002/fld

4. Scardovelli R, Zaleski S. Direct numerical simulation of free-surface and interfacial flow. *Annual Review of Fluid Mechanics* 1999; **31**:567–603.
5. López J, Hernández J, Gómez P, Faura F. A volume of fluid method based on multidimensional advection and spline interface reconstruction. *Journal of Computational Physics* 2004; **195**:718–742.
6. Bussmann M, Chandra S, Mostaghimi J. Modeling the splash of a droplet impacting a solid surface. *Physics of Fluids* 2000; **12**:3121–3132.
7. Li J, Renardy YY, Renardy M. Numerical simulation of breakup of a viscous drop in simple shear flow through a volume-of-fluid method. *Physics of Fluids* 2000; **12**:269–282.
8. Liu PL-F, Wu T-R, Raichlen F, Synolakis C, Borrero J. Runup and rundown generated by three-dimensional sliding masses. *Journal of Fluid Mechanics* 2005; **536**:107–144.
9. Benson DJ. Volume of fluid interface reconstruction methods for multi-material problems. *Applied Mechanics Review* 2002; **55**:151–165.
10. Bell RL, Hertel ES. An improved material interface reconstruction algorithm for Eulerian codes. *Technical Report SAND92-1716*, Sandia National Laboratories, 1992.
11. Mosso S, Clancy S. A geometrically derived priority system for Youngs' interface reconstruction. *Technical Report*, Los Alamos National Laboratory, 1994.
12. Benson DJ. Eulerian finite element methods for the micromechanics of heterogeneous materials: dynamic prioritization of material interfaces. *Computer Methods in Applied Mechanics and Engineering* 1998; **151**: 343–360.
13. Parker BJ, Youngs DL. Two and three dimensional Eulerian simulation of fluid flow with material interfaces. *Technical Report 01/92*, UK Atomic Weapons Establishment, 1992.
14. Pilliod Jr JE, Puckett EG. Second-order accurate volume-of-fluid algorithms for tracking material interfaces. *Journal of Computational Physics* 2004; **199**:465–502.
15. Press WE, Flannery BP, Teukolsky SA, Vetterling WT. *Numerical Recipes*: *The Art of Scientific Computing* (2nd edn). Cambridge University Press: Cambridge, 1992.
16. Rudman M. Volume-tracking methods for interfacial flow calculations. *International Journal of Numerical Methods Fluids* 1997; **24**:671–691.

DOI: 10.1002/fld